EXTRACTION OF FEATURES FROM OBJECTS IN URBAN AREAS USING SPACE-TIME ANALYSIS OF RECORDED LASER PULSES

B. Jutzi [a], U. Stilla [b]

[a] FGAN-FOM Research Institute for Optronics and Pattern Recognition, 76275 Ettlingen, Germany - jutzi@fom.fgan.de

[b] Photogrammetry and Remote Sensing, Technische Universitaet Muenchen, 80290 Muenchen, Germany - stilla@bv.tum.de

Commission II, WG II/2

KEY WORDS: Urban, Analysis, Simulation, Laser scanning, LIDAR, Measurement, Feature.

ABSTRACT:

In this paper we describe a simulation system and investigations for analysis of recorded laser pulses. A simulation setup that considers simulated signals of synthetic objects was developed for exploring the capabilities of recognizing urban objects using a laser system. The temporal waveform of each laser pulse is analyzed for gaining the pulse properties: range, pulse power and number of peaks. Considering the received pulse power of the associated spatial neighborhood for the region boundary delivers the estimation of the edge position and edge orientation with sub pixel accuracy.

1. INTRODUCTION

The automatic generation of 3-d models for a description of man-made objects, like buildings, is of great interest in photogrammetric research. In photogrammetry a spatial surface is classically measured by triangulation of corresponding image points from two or more pictures of the surface. The points are manually chosen or automatically detected by analyzing image structures. Besides this indirect measurement using object characteristics, which depends on natural illumination, active laser scanner systems allow a direct and illumination-independent measurement of the range. Laser scanners capture the range of 3-d objects in a fast, contactless and accurate way. Overviews for laser scanning systems are given in (Huising & Pereira, 1998; Wehr & Lohr, 1999; Baltsavias, 1999).

Current pulsed laser scanner systems for topographic mapping are based on time-of-flight ranging techniques to determine the range of the illuminated object. The time-of-flight is measured by the elapsed time between the emitted and backscattered laser pulses. The signal analysis to determine the elapsed time typically operates with analogous threshold detection (e.g. peak detection, leading edge detection, constant fraction detection). Some systems capture multiple reflections, caused by objects which are smaller than the footprint located in different ranges. Such systems usually capture the first and the last backscattered laser pulse (Baltsavias, 1999). Currently first pulse as well as last pulse exploitation is used for different applications like urban planning or forestry surveying. While first pulse registration is the optimum choice to measure the hull of partially penetrable objects (e.g. canopy of trees), last pulse registration should be chosen to measure non-penetrable surfaces (e.g. ground surface). Figure 1a shows a section of an image taken in first pulse mode. The foliage of the trees is visible. Figure 1b was taken in last pulse mode. The branches and foliage are not visible and the building areas are smaller than in Figure 1a. Due to multiple pulse reflection at the boundary of the buildings and the processing by first or last pulse mode, building areas dilate or erode. For visualizing the various sizes of the building footprints in first and last pulse images a difference image is calculated (Figure 1c). The ambiguous pixels of the building are visible by a bright area along the buildings contours. A zoomed section of a building corner is depicted in Figure 1d. Building edges are expected within these bright areas.

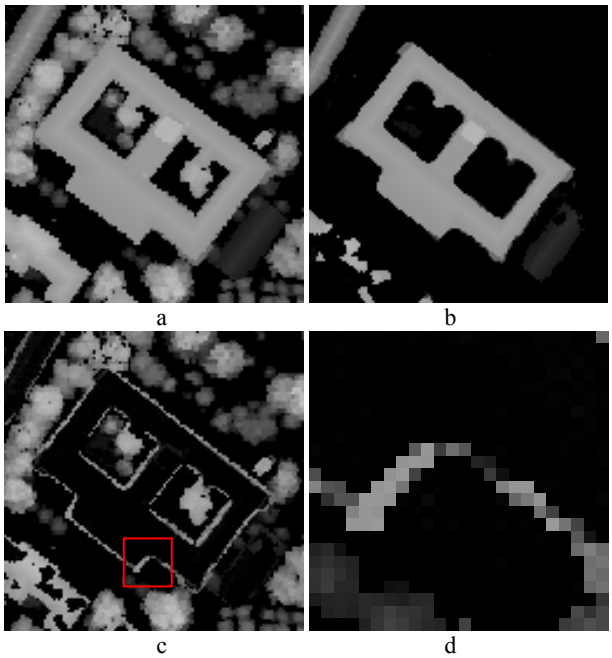

Figure 1. Sections of an urban scene (Test area Karlsruhe, Germany).
a) elevation images captured by first pulse mode,
b) elevation images captured by last pulse mode,
c) difference image of first and last pulse mode,
d) subsection of the difference image (building boundary).

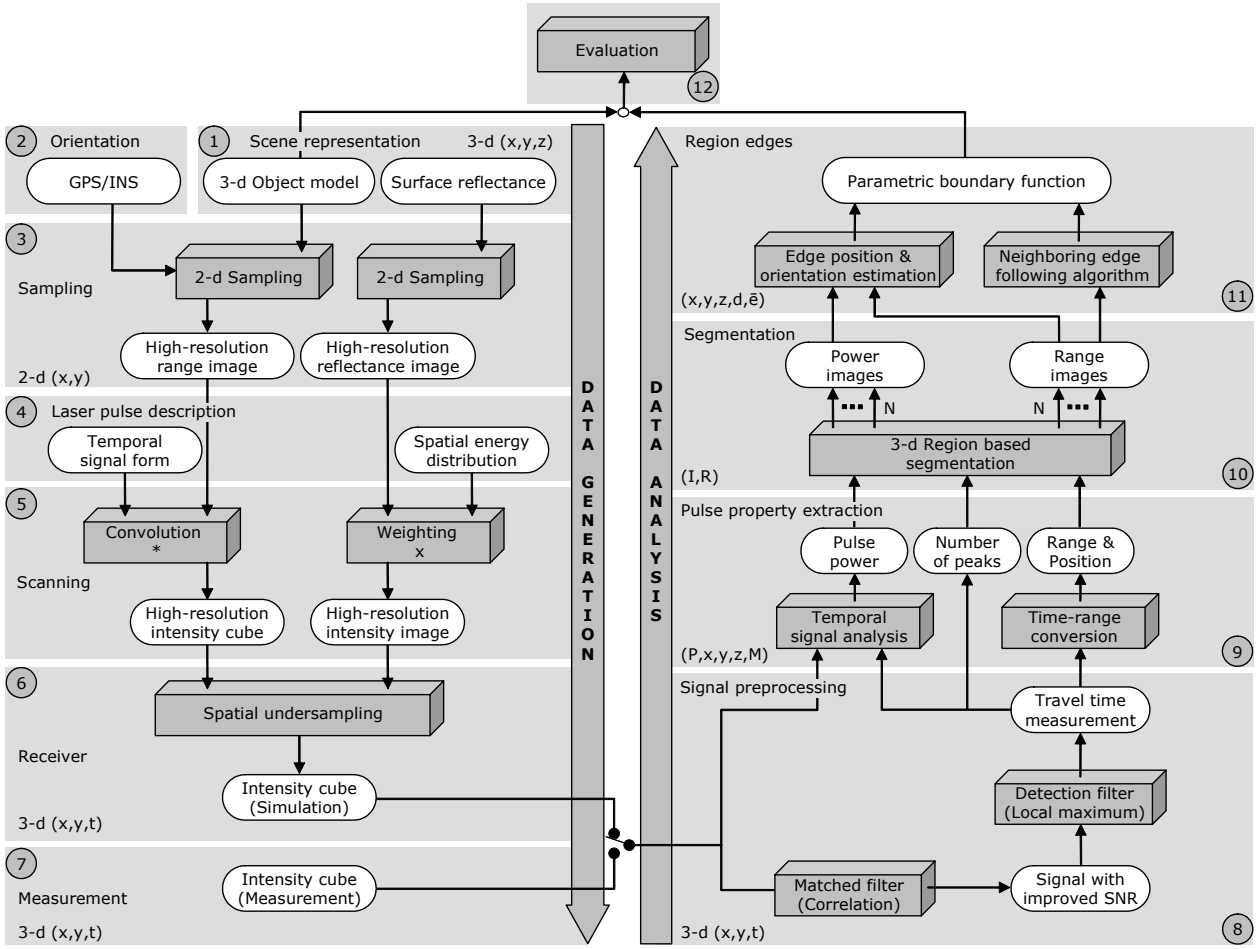

Figure 2. Simulation setup: data generation (left), and analysis (right)

Beside the first or last pulse exploitation the complete waveform in between might be of interest, because it includes the backscattering characteristic of the illuminated field. Investigations on analyzing the waveform were done to explore the vegetation concerning the bio mass, foliage or density (e.g. trees, bushes, and ground). NASA has developed a prototype of a Laser Vegetation Imaging Sensor (LVIS) for recording the waveform to determine the vertical density profiles in forests (Blair *et al.*, 1999). The spaceborne Geoscience Laser Altimeter System (GLAS) determines distance to the Earth's surface, and a profile of the vertical distribution of clouds and aerosols. In some applications (e.g. observation of climate changes), clouds are objects of interest. But, clouds can also be considered as obstacles, which limit the visibility of the illuminated object.

Apart from the range measurement of laser scanner systems some systems deliver a single reflectance value derived from the intensity or the power of the backscattered laser light. The intensity is determined by the signal maximum and the power by signal integration of the measured laser light and gives radiometric information about the surveyed area. This intensity (power) value can be used for separating segments of artificial objects from vegetation (Hug & Wehr, 1997; Maas, 2001) or perfectly textured 3-d scene models (Sequeira *et al.*, 1999). Vosselman (2002) suggested considering the reflectance strength of the laser beam response to estimate and improve the accuracy of reflectance edge positions.

In this paper we describe a simulation system and investigations for analysis of recorded laser pulses. In Section 2 a short overview on the simulation setup we used is described. The data generation is presented in Section 3. In Section 4 the processing chain for the data analysis is explained.

2. OVERVIEW OF THE SIMULATION SETUP

We focus on the aforementioned problem of measurement situations on building boundaries. A simulation setup that considers simulated signals of synthetic objects was build up for exploring the capabilities of recognizing urban objects using a laser system. The simulation setup is split in *data generation* which is described in Section 3 and *data analysis* in Section 4. A schematic illustration of the simulation setup is depicted in Figure 2.

The *data generation* can be carried out by a simulation or a measurement of the temporal waveform. By the use of a 3-d *scene representation* for the building model (Figure 2-1) and the *extrinsic orientation* parameter for sensor position and orientation (Figure 2-2), the model is *sampled* to get a high-resolution range and reflectance image (Figure 2-3). The resolution has to be higher than the scanning grid we want to simulate for further processing. Considering the temporal and spatial *laser pulse description* is relevant for modeling the laser pulse (Figure 2-4). To simulate the *scanning* of the laser system, the values of grid spacing and the divergence of the

laser beam are used for convolving the high-resolution range image with the temporal waveform and weighting the high-resolution reflectance image with the spatial energy distribution (Figure 2-5). The spatial undersampling of the high resolution data is comparable to focusing the laser beam on the detector of the *receiver* (Figure 2-6). This kind of processing generates an intensity cube where the values correspond to the intensity of the signal. The simulation should give a realistic description of what we would expect from the measurement (Figure 2-7).

To improve the estimate of the building's edge position the intensity cube is processed (*data analysis*). Processing starts with the matched filtering for *signal preprocessing* of the intensity cube to increase the accuracy of the range measurement and improve the detection rate (Figure 2-8). Then each detected pulse is investigated for characteristic properties with *pulse property extraction* to get an enhanced description of the illuminated surface (Figure 2-9). By the use of the determined pulse properties a region based *segmentation* algorithm generates range and power images for region descriptions to handle the ambiguity of multiple reflections at the same spatial position (Figure 2-10). Analyzing the pulse power in the associated spatial neighborhood of the *region edges* estimates the edge position and edge orientation with sub pixel accuracy (Figure 2-11). Finally, for evaluation the received parametric boundary function of the region edges has to be compared with the 3-d object model (Figure 2-12).

3. DATA GENERATION

For simulating the temporal waveform of the backscattered pulses a *scene model* (i) and a *sensor model* (ii) is required.

3.1 Scene modeling

3.1.1 Scene representation

For a 3-d scene representation, our simulation setup considers geometric and radiometric features of the illuminated surface in the form of 3-d object models with homogeneous surface reflectance. Figure 3 shows a 3-d object model with a homogeneous surface reflectance of the building in Figure 1 based on VRML (Virtual Reality Modeling Language).

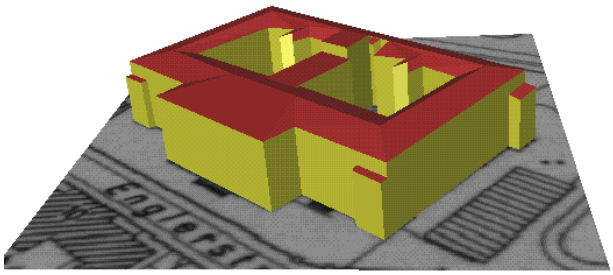

Figure 3. 3-d object model with homogeneous surface reflectance

3.1.2 Sampling

The object model with homogeneous surface reflectance is then sampled higher than the scanning grid we simulate and process, because with the higher spatial resolution we simulate the spatial distribution of the laser beam. Considering the position and orientation of the sensor system we receive a high-resolution range image (Figure 4) and reflectance image. Depending on the predetermined position and orientation of the sensor system, various range images can be captured.

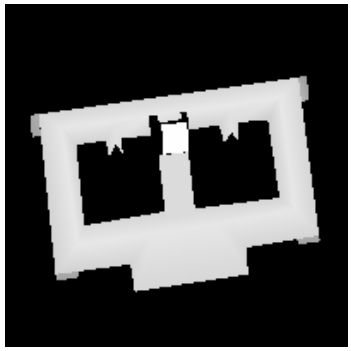

Figure 4. High-resolution range image

3.2 Sensor modeling

The sensor modeling considers the specific properties of the sensing process: the position and orientation of the sensor, the laser pulse description, scanning and the receiver properties.

3.2.1 Orientation

To simulate various aspects a description of the extrinsic orientation of the laser scanning system with a GPS/INS system is used.

3.2.2 Laser pulse description

The transmitted laser pulse of the system is characterized by specific pulse properties (Jutzi et al., 2003a). We assume a radial symmetric Gaussian spatial distribution and a temporal exponential function as an approximation for the laser pulse.

3.2.3 Scanning

Depending on the scan pattern of the laser scanner system, the grid spacing of the scanning and the divergence of the laser beam a sub-area of the high-resolution range image is processed. By convolving the sub-area of the range image with the temporal waveform of the laser pulse, we receive a high-resolution intensity cube. Furthermore the corresponding sub-area of the high-resolution reflectance image is weighted with the spatial energy distribution of the laser beam (Gaussian distribution at the grid line $\pm 2\sigma$) to take into account the amount of backscattered laser light for each reflectance value. Then we have a description of the backscattered laser beam with a higher spatial resolution than necessary for processing.

3.2.4 Receiver

By focusing the beam with its specific properties on the detector of the receiver, the spatial resolution is reduced and this is simulated with a spatial undersampling of the sub-areas.

Finally we receive an intensity cube that considers the scanning width of the simulated laser scanner system and the temporal description of the backscattered signal. Because each reflectance value in the sub-area is processed by undersampling, multiple reflections are considered with the backscattered signal.

4. DATA ANALYSIS

Algorithms are developed and evaluated with simulated signals of synthetic objects.

First, a signal preprocessing of the intensity cube with a matched filter is implemented to increase the precision of the range measurement and improve the detection rate. These results are used to analyze the waveform of each pulse for gaining the pulse properties: range, pulse power and number of peaks. Then the pulse properties are processed with a region based segmentation algorithm. By the use of images the region boundary pixels derived from multiple reflections at the same spatial position are shared by separate regions. Considering the received pulse power of the associated spatial neighborhood for the region boundary delivers the estimation of the edge position and edge orientation with sub pixel accuracy.

4.1 Signal preprocessing

The data analysis starts with the detection of pulses in the temporal signal of the intensity cube. Usually this signal is disturbed by various noise components: background radiation, amplifier noise, photo detector noise etc. Detecting the received signal of the pulse in noise and extracting the associated travel time of the pulse is a well-known problem and is discussed in detail in radar techniques (Mahafza, 2000; Osche, 2002; Skolnik, 1980) and system theory (Papoulis, 1984; Turin, 1960; Unbehauen, 1996). Due to this problem matched filters are used.

To improve the range accuracy and the signal-to-noise ratio (*SNR*) the matched filter for the signal of the backscattered pulse has to be determined. In practice, it is difficult to determine the optimal matched filter. In cases where no optimal matched filter is available, sub-optimum filters may be used, but at the cost of decreasing the SNR. With the assumption that the temporal deformation of the received signal can be neglected and the waveform is uniformly attenuated (isotropic attenuation by reflection or transmission of the pulse) the signal of the emitted pulse is the best choice for the matched filter determination.

Let us further assume that the noise components of the system mentioned above are sufficiently described by white noise with the constant factor N_0. Furthermore the signal energy of the pulse is known as E, and the maximum *SNR* occurs if the signal and the filter match. In this case the associated travel time t of the delayed pulse is t_0 and the *SNR* is described by

$$SNR(t_0) = \frac{2E}{N_0} \tag{1}$$

An interesting fact of this result is that the maximum of the instantaneous *SNR* depends only on the signal energy of the emitted pulse and the noise, and is independent of the waveform.

The matched filter is computed by the cross-correlation R_{XS} between the signal of the emitted pulse x and the received signal s. We obtain the output signal y with a local maximum at the delay time τ.

$$y(t) = R_{xs}(t - \tau) \tag{2}$$

Then the output signal with improved SNR is analyzed by a detection filter for local maxima to determine the travel time of the pulse. By using the correlation signal for processing the travel time a higher accuracy is reached than by operating on the waveform. This is because the specific pulse properties (e.g. asymmetric shape, spikes) are taken into account and so less temporal jitter can be expected. For the detection the preservation of the waveform has no relevance, only maximizing the *SNR* is important.

Furthermore, the range resolution of the laser scanning system generally depends on the temporal width of the emitted pulse. Short pulses decrease the average signal power and the associated *SNR*. To increase the temporal pulse width T without decreasing range resolution we need to consider pulse compression. The typical time-bandwidth product of a conventional system is $BT \approx 1$, but with an increasing bandwidth B of the receiver and a corresponding waveform the range resolution ΔR is improved and we obtain with the speed of light c

$$\Delta R = \frac{c}{2B} . \tag{3}$$

Then the improved range resolution of the laser scanner system is inversely proportional to the bandwidth.

4.2 Pulse property extraction

Depending on the size of the focused surface geometry in relation to the laser beam (footprint and wavelength) different properties can be extracted (Jutzi & Stilla, 2003b). In this paper we focus on the properties range, pulse power and number of peaks.

- The range value is processed to determine the distance from the system to the illuminated surface.
- The pulse power value is computed to get a description for the reflectance strength of the illuminated area.
- The number of peaks is considered to locate the boundaries of an object with multiple reflections.

For determining the property values of each pulse the intensity cube is processed in different ways. First the range value is found from the measured travel time of pulse by the matched filter. Then the travel time is used to locate the area of interest in the intensity cube for temporal signal analysis. We integrate this area with the received signal s for the pulse power value P

$$P = \frac{1}{2T} \int_{-T}^{T} s^2(t) dt . \tag{4}$$

Integrating the intensity over a small area instead of quantizing a single value has the advantage of decreasing the noise influence (Vosselman, 2002).

Finally the number of peaks is determined by the number of detected reflections for each emitted pulse. The number of detected pulses depends on the threshold adjustment for the local maximum detection of the matched filter output signal.

4.3 Segmentation

The segmentation of the range values provides a higher level model formation. Segmentation considers the spatial neighborhood of detected pulses to generate surface primitives

in the form of regions. Separating the pulse properties range and power in regions is fundamental to handling the ambiguity of multiple reflections at the same spatial position. Boundary pixels are labeled as shared pixels belonging to background and foreground. Figure 6 illustrates the region definition.

The computed region N consisting of range values is described by the range image R_N. Then the pulse power values of the same pulses are used to generate the power image I_N. In this manner we receive a corresponding representation of all determined regions ($N = 1, 2, 3, \ldots$).

The region boundary mainly contains pixels derived from multiple reflections. The region interior is characterized by single reflections and fills up the region to the boundary. The region background is labeled with zero pixel values. Generally it can be said that nonzero pixels belong to the region and zero pixels constitute the background.

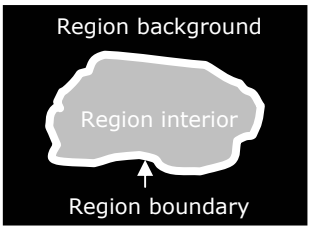

Figure 6. Region components definition

An iterative region growing algorithm considers the range properties of all pulses in the spatial neighborhood: if the range difference of a pulse and the proofing pulse is below a given threshold, then the pulse is connected and grouped as a new element to this region. Samples of range and power images as segmentation results are depicted in Figure 7.

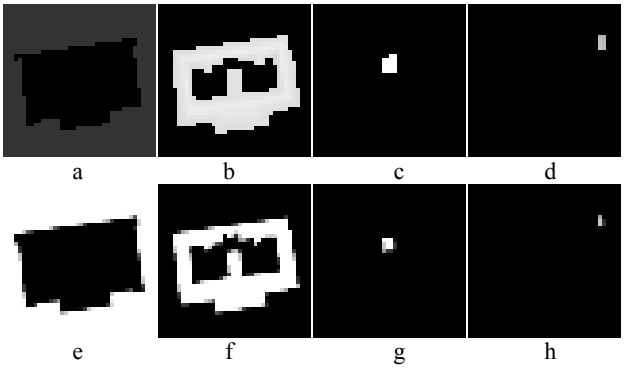

Figure 7. Segmentation results (grid mesh width g=275cm, Gaussian distribution of the beam at the grid line ±2σ): a)-d) range image $R_{N=1}$, $R_{N=2}$, $R_{N=3}$, $R_{N=4}$, e)-h) power image $I_{N=1}$, $I_{N=2}$, $I_{N=3}$, $I_{N=4}$

4.4 Region edges

For physical edge description a data driven region boundary (edges) approach similar to the algorithm of Besl (1988) is used. This approach generates a parametric function representation of the region boundary for higher level processing. To refine the region boundary the estimation of edge position and edge orientation from received pulse power and analysis of the spatial neighborhood is proposed.

First each power image I_N is processed with a 4-neighboring edge following algorithm to determine a parametric function representation of the region boundary. The algorithm traces the exterior boundary of the region N in the power image $I_N(x,y)$. As output for each trace, we construct two boundary parameterization functions $x_N(s)$ and $y_N(s)$ containing the row and column coordinates of the connected boundary pixels. Additionally the boundary range function $z_N(s)$ can be found using the range image.

Figure 8 shows an example of an exterior edge description with the three parameter boundary functions $x_{N=2}(s)$, $y_{N=2}(s)$, $z_{N=2}(s)$ of the region N=2 and corresponding power image I_N with overlaid boundary.

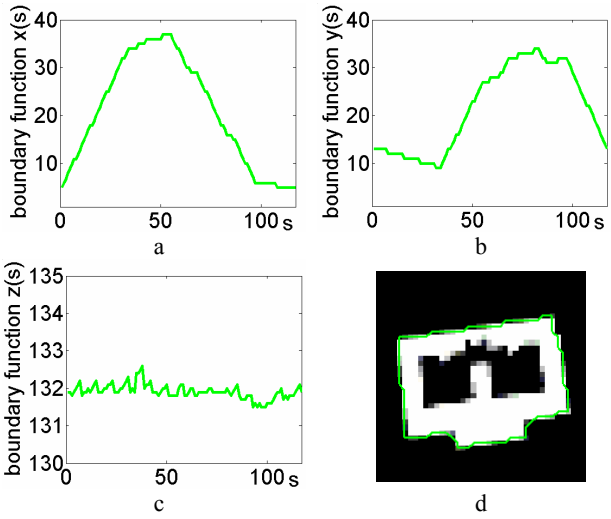

Figure 8. Edge description: parameter functions a) $x_{N=2}(s)$, b) $y_{N=2}(s)$, c) $z_{N=2}(s)$, d) power image $I_{N=2}$ with overlaid outer boundary function

Figure 9a shows a 3-by-3 pixel neighborhood including a region boundary labeled E, the region interior I and the region background B. By assuming a straight edge from the upper left pixel to the center pixel the line is undetermined without further information. A sample of possible edges $\bar{e}_1$, $\bar{e}_2$ and $\bar{e}_3$ is depicted.

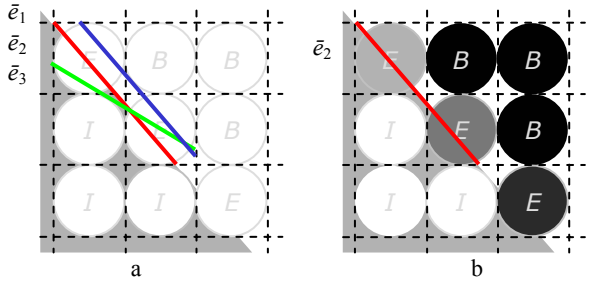

Figure 9. Edge estimation a) sample of edges $\bar{e}_1$, $\bar{e}_2$ and $\bar{e}_3$, b) estimated edge $\bar{e}_2$

To estimate the edge position and edge orientation the received pulse power is analyzed for the geometrical shape of the illuminated surface. With the assumption of a uniform reflectance property of the surface the target reflectance depends only on the geometrical shape. Therefore we assume uniform reflectance and straight object edges. The laser beam with its radial symmetric Gaussian distribution illuminates an edge. For integrating along the coordinate we assume the edge is vertical. Furthermore the beam center distance to the edge $\bar{e}$ is given by d (Figure 10).

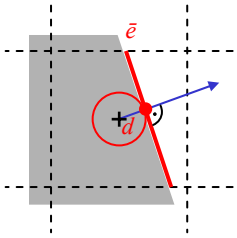

Figure 10. Edge $\bar{e}$ with distance d

If the area to the left (region interior) has a high reflectance of 100 % and the area to the right (region background) has a low reflectance of 0 %, then we derive for the boundary pulse power as function of d

$$P_B(d) = \frac{1}{\pi\sigma^2}\int_{-\infty}^{\infty}\int_{-\infty}^{d} e^{-\frac{x^2+y^2}{\sigma^2}}\,dx\,dy = \frac{1}{\sqrt{\pi\sigma^2}}\int_{-\infty}^{d} e^{-\frac{x^2}{\sigma^2}}\,dx \quad (5)$$

For horizontal edges the boundary pulse power is derived in the same way. Since we assumed a uniform reflectance property of the surface, the reflectance is a linear function of the distance d and only valid if d is inside the mesh of the boundary pixel area. By this observation the distance d between the estimated edge and the beam center is fixed, whereas the edge orientation remains to be found.

To achieve this we analyze the spatial edge neighborhood. There we receive another estimated edge as the tangent of a circle. Assuming again a straight edge, four tangents on the two circles are found. For circles at (0/0) and (g/0) with radius d_1 and d_2 we see:

$$\bar{x}\,\bar{n} = d_1 \quad \text{with} \quad \bar{n} = \begin{pmatrix} -\dfrac{d_2 \pm d_1}{g} \\ \sqrt{1-\dfrac{(d_2 \pm d_1)^2}{g^2}} \end{pmatrix}. \quad (6)$$

Due to this the constraint of the region interior or region background in the spatial neighborhood is used for a unique position and orientation of the edge. Figure 9b sketches the estimated edge derived from the power values of two pixels. The brightness of the pixels shows the power values.

This model is now correct for essentially straight edges. Obviously the model is incorrect for corners, so these will have to be determined by extrapolating adjoining edges.

5. CONCLUSION

The space-time analysis of recorded laser pulses allows a sub pixel estimation of the edge. Only two pulse power values of the boundary with respect to the spatial neighborhood are necessary for a unique estimation of the edge position and orientation. For processing the intensity cube an adaptive threshold operation is possible and it allows exploiting different features without selecting a special feature in advance. The simulation was helpful for develop algorithms. The data generation and analysis we carried out are general investigations for a laser system which records the waveform of laser pulses. Future work focuses on an improved analysis of the received signal.

6. ACKNOWLEDGEMENT

The authors would like to thank Jörg Neulist for his fruitful discussions during the preparation of this work.

REFERENCES

Baltsavias EP (1999) Airborne laser scanning: existing systems and firms and other resources. ISPRS Journal of Photogrammetry & Remote Sensing 54: 164-198.

Besl PJ (1988) *Surfaces in Range Image Understanding*. New York: Springer-Verlag.

Blair JB, Rabine DL, Hofton MA (1999) The Laser Vegetation Imaging Sensor (LVIS): A medium-altitude, digitization-only, airborne laser altimeter for mapping vegetation and topography. ISPRS Journal of Photogrammetry & Remote Sensing 56: 112-122.

Hug C, Wehr A (1997) Detecting and identifying topographic objects in laser altimeter data. ISPRS, International Archives of Photogrammetry & Remote Sensing, Vol. 32, Part 3-4W2: 19-26.

Huising EJ, Gomes Pereira LM (1998) Errors and accuracy estimes of laser data acquired by various laser scanning systems for topographic applications. ISPRS Journal of Photogrammetry & Remote Sensing 53: 245-261.

Jutzi B, Eberle B, Stilla U (2003a) Estimation and measurement of backscattered signals from pulsed laser radar. In: Serpico SB (ed) Image and Signal Processing for Remote Sensing VIII, SPIE Proc. Vol. 4885: 256-267.

Jutzi B, Stilla U (2003b) Analysis of laser pulses for gaining surface features of urban objects. 2nd GRSS/ISPRS Joint Workshop on Remote Sensing and data fusion on urban areas, URBAN 2003: 13-17.

Maas HG (2001) The suitability of airborne laser scanner data for automatic 3D object reconstruction. In: Baltsavias EP, Gruen A, Van Gool L (eds) Automatic Extraction of Man-Made Objects From Aerial and Space Images (III), Lisse: Balkema.

Mahafza BR (1998) *Introduction to Radar Analysis*. Boca Raton, FL: CRC Press.

Osche GR (2002) *Optical Detection Theory for Laser Applications*. N.J.: Wiley-Interscience.

Papoulis A (1984) *Probability, Random Variables, and Stochastic Processes*. Tokyo: McGraw-Hill.

Sequeira V, Ng KC, Wolfart E, Gonçalves JGM, Hogg DC (1999) Automated Reconstruction of 3D Models from Real Environment, ISPRS Journal of Photogrammetry & Remote Sensing 53: 1–22.

Skolnik MI (1980) *Introduction to radar systems*. McGraw-Hill International Editions, Second Edition.

Turin GL (1960) An introduction to matched filters, IEEE Trans. Info. Theory, vol. IT-6, 311-329.

Unbehauen R (1996) *Systemtheorie 1*. Oldenbourg Verlag, München, 7. Auflage.

Vosselman G (2002) On estimation of planimetric offsets in laser altimetry data. Vol. XXXIV, International Archives of Photogrammetry and Remote Sensing: 375-380.

Wehr A, Lohr U (1999) Airborne laser scanning – an introduction and overview. ISPRS Journal of Photogrammetry & Remote Sensing 54: 68-82.